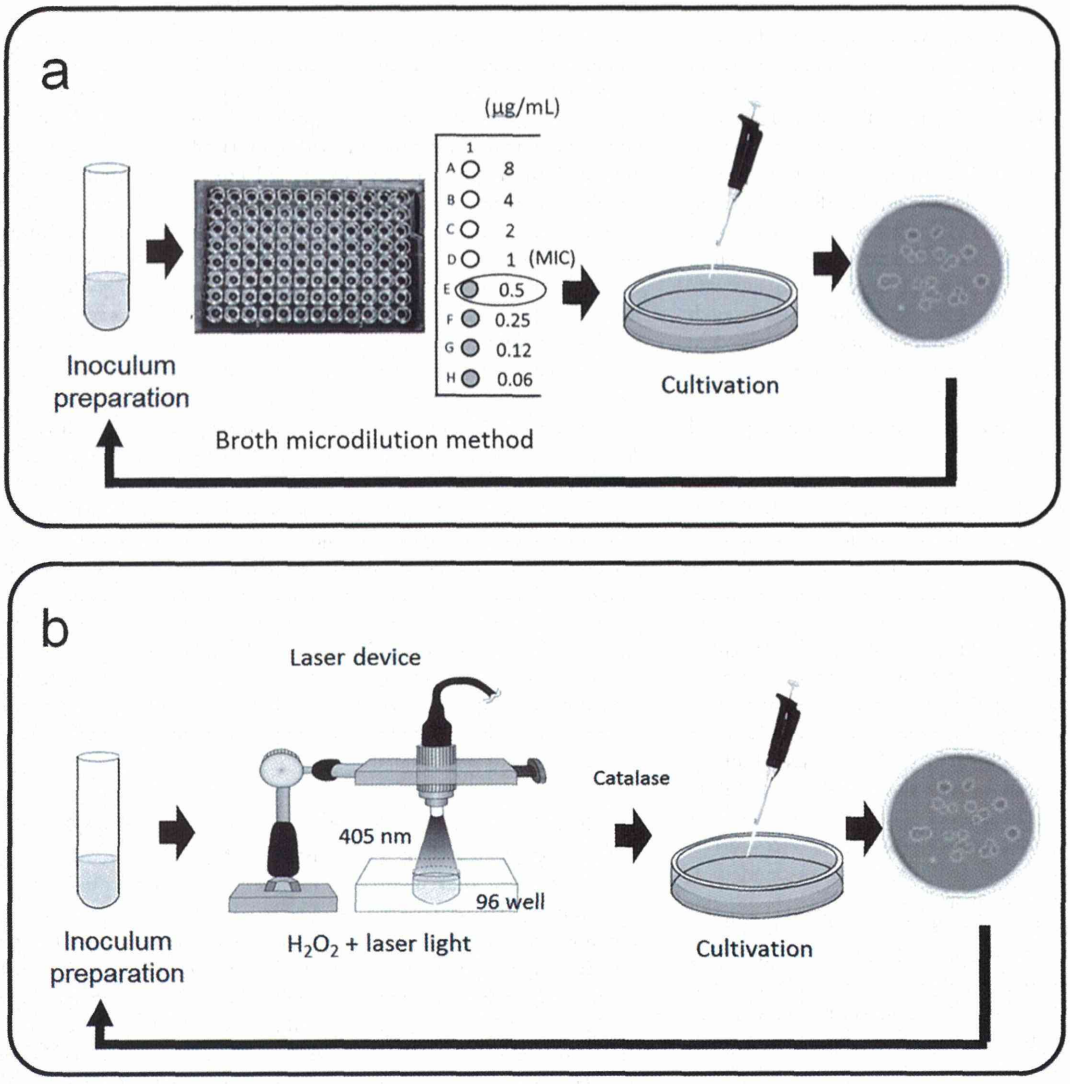

Figure 1. Schematic illustrations of susceptibility testing. (a) Antibacterial agents and (b) disinfection treatment with photolysis of H_2O_2 are shown.
doi:10.1371/journal.pone.0081316.g001

agents against *E. faecalis* and *E. coli* were within a rather wide range (0.5 to 16 μg/mL against *E. faecalis*, and 0.015 to 128 μg/mL against *E. coli*). Prominent increases in MIC were observed in CFPN against *E. faecalis* (from 8 μg/mL at the initial to 128 μg/mL at the tenth) and MINO against *E. coli* (from 0.5 μg/mL at the initial to 16 μg/mL at the tenth). Regarding MICs against *S. salivarius*, MICs of CFPN and MINO could not be obtained because no visible bacterial growth was observed even at the lowest concentration of each agent. Of the seven antibacterial agents, only the MIC of AMX showed 4 times increase during the experiment.

To figure out the entire spectrum of inducing bacterial resistance, Fig. 2 shows the changes in the fold increase in MIC in which each initial MIC is regarded as 1 MIC. Of the four bacterial species tested, susceptibility of *S. aureus* prominently lowered with the number of treatment, and all the seven antibacterial agents induced 4- or higher fold increases in MIC. Susceptibility of *E. faecalis* and *E. coli* also lowered in some of the antibacterial agents with the number of treatment. AMX, CFPN, EM, and MINO induced 4- or higher fold increases in MIC against *E. faecalis*, and OFLX and MINO against *E. coli*. Susceptibility of *S. salivarius* tended to be rather stable as compared to that of the other bacterial strains during the experiment.

Susceptibility testing for disinfection treatment with photolysis of H_2O_2

Figure 3 shows the changes in the antibacterial effect of repeated disinfection treatment with photolysis of H_2O_2 in four bacterial species, *S. aureus*, *E. faecalis*, *E. coli*, and *S. salivarius*. When each bacterial species was exposed to the first treatment with photolysis of H_2O_2, an approximate 2-log reduction in viable counts was observed. Repeated exposure of bacteria to the treatment of photolysis of H_2O_2 did not affect bacterial susceptibility. In addition, the magnitude of the reduction in viable counts in any of the bacterial species tested was mostly within the range of 2- to 3-log order during repeated treatment up to 40 times. Figure 4 shows the changes in the antibacterial effect of repeated disinfection treatment with photolysis of H_2O_2 in the three bacterial species, *P. aeruginosa*, *S. mutans*, and *A. actinomycetemcomitans*. Similar to the other four bacterial species described

Table 1. MICs on the first, fifth, and tenth exposure of each bacterial species to antibacterial agents.

Staphylococcus aureus				Enterococcus faecalis			
Drug	MIC (μg/mL)			Drug	MIC (μg/mL)		
	Initial	5th	10th		Initial	5th	10th
AMX*	0.12	1	2	AMX*	0.5	1	2
CFPN*	0.5	128	128	CFPN*	8	128	128
EM*	0.5	4	8	EM*	2	4	8
OFLX*	0.5	4	4	OFLX	2	4	4
CLDM*	0.25	16	32	CLDM	16	16	32
CPFX*	0.5	2	2	CPFX	1	2	2
MINO*	0.25	2	8	MINO*	2	8	16
Escherichia coli				**Streptococcus salivarius**			
Drug	MIC (μg/mL)			Drug	MIC (μg/mL)		
	Initial	5th	10th		Initial	5th	10th
AMX	4	8	8	AMX*	0.03	0.03	0.12
CFPN	1	2	2	CFPN	<0.015	<0.015	<0.015
EM	32	64	64	EM	0.06	0.06	0.12
OFLX*	0.06	0.12	0.48	OFLX	2	4	4
CLDM	128	128	128	CLDM	0.06	<0.015	<0.015
CPFX	0.015	<0.015	<0.015	CPFX	1	2	2
MINO*	0.5	4	16	MINO	<0.12	<0.12	<0.12

Each value represents the mean of duplicate determinations.
Asterisks indicate induction of bacterial resistance to corresponding antibacterial agents as defined by an increase of four times or more in MIC over the initial MIC.
doi:10.1371/journal.pone.0081316.t001

above, an approximate 2-log reduction in viable counts was observed at the first exposure of each bacterial species to treatment with photolysis of H_2O_2. Of the three bacterial species, *P. aeruginosa* and *A. actinomycetemcomitans* showed a relatively high susceptibility to this treatment because a laser light irradiation time as short as 10 s for *P. aeruginosa* and 30 s for *A. actinomycetemcomitans*, was sufficient for achieving a 2-log reduction in viable counts. Repeated exposure of these two bacterial species to treatment with photolysis of H_2O_2 resulted in a relatively large fluctuation in the antibacterial effect compared with *S. mutans* and the four bacterial species (*S. aureus*, *E. faecalis*, *E. coli*, and *S. salivarius*) shown in Figure 3. However, even in the two species *P. aeruginosa* and *A. actinomycetemcomitans*, no development of bacterial resistance to treatment of photolysis of H_2O_2 was observed during 40 times of exposure. For *S. mutans*, as was the case with the former four bacterial species (*S. aureus*, *E. faecalis*, *E. coli*, and *S. salivarius*), the magnitude of reduction in viable counts hardly deviated from the range of 2- to 3-log order during repeated treatment up to 40 times.

Quantification of hydroxyl radicals generated by photolysis of H_2O_2

Laser irradiation of H_2O_2 generated an ESR signal of DMPO-OH. The presence of the spin adduct was confirmed by hyper fine coupling constants of $a_N = a_H = 1.49$ mT for DMPO-OH [17]. The yield of DMPO-OH increased linearly with the laser irradiation time, and the generation rates of DMPO-OH (slope values of lines) also increased with the concentration of H_2O_2 (Fig. 5). When H_2O_2 at concentrations of 250, 500, and 1000 mM was irradiated with the laser light for 30 s, the yields of DMPO-OH were 12.8, 22.5, and 41.6 mM, respectively.

Discussion

The present study showed that repeated exposure of bacteria to disinfection treatment with photolysis of H_2O_2 did not induce bacterial resistance to this treatment. With regard to the antibacterial agents tested, in all of the agents tested, at least one of the four bacterial species resistant to the agents was observed with repeated exposure. As mentioned above, monitoring MICs of the agents after serial passage of the culture through subinhibitory concentrations of the agents has proven effective for assessing the risk of developing bacterial resistance [11–13]. Bacteria were cultivated under drug-free conditions prior to each susceptibility assay in the present study (Fig. 1a). The setup of the assay protocol was designed in this manner to be in accordance with susceptibility testing for disinfection treatment with photolysis of H_2O_2. Because continuous or serial exposure of bacteria to treatment with photolysis of H_2O_2 would cause a lethal effect, the serial passage technique could not be applied. Therefore, bacteria were cultivated prior to each susceptibility assay under partially bactericidal conditions, which were obtained by adjusting the laser light irradiation time (Fig. 1b). Even when cultivation was performed in advance between each susceptibility assay, repeated exposure of bacteria to subinhibitory concentrations of antibacterial agents resulted in development of bacteria that were resistant to the agents. Of the four bacterial species tested, increases in MICs were more prominent in *S. aureus* and *E. faecalis* than in *E. coli* and *S. salivarius*. The reason for the difference in the magnitude of drug-resistance induction among bacterial species cannot be explained at the present time. In addition, only one strain for each bacterial species was tested. Therefore, the conclusion that this difference was species dependent cannot be made. Nonetheless, to

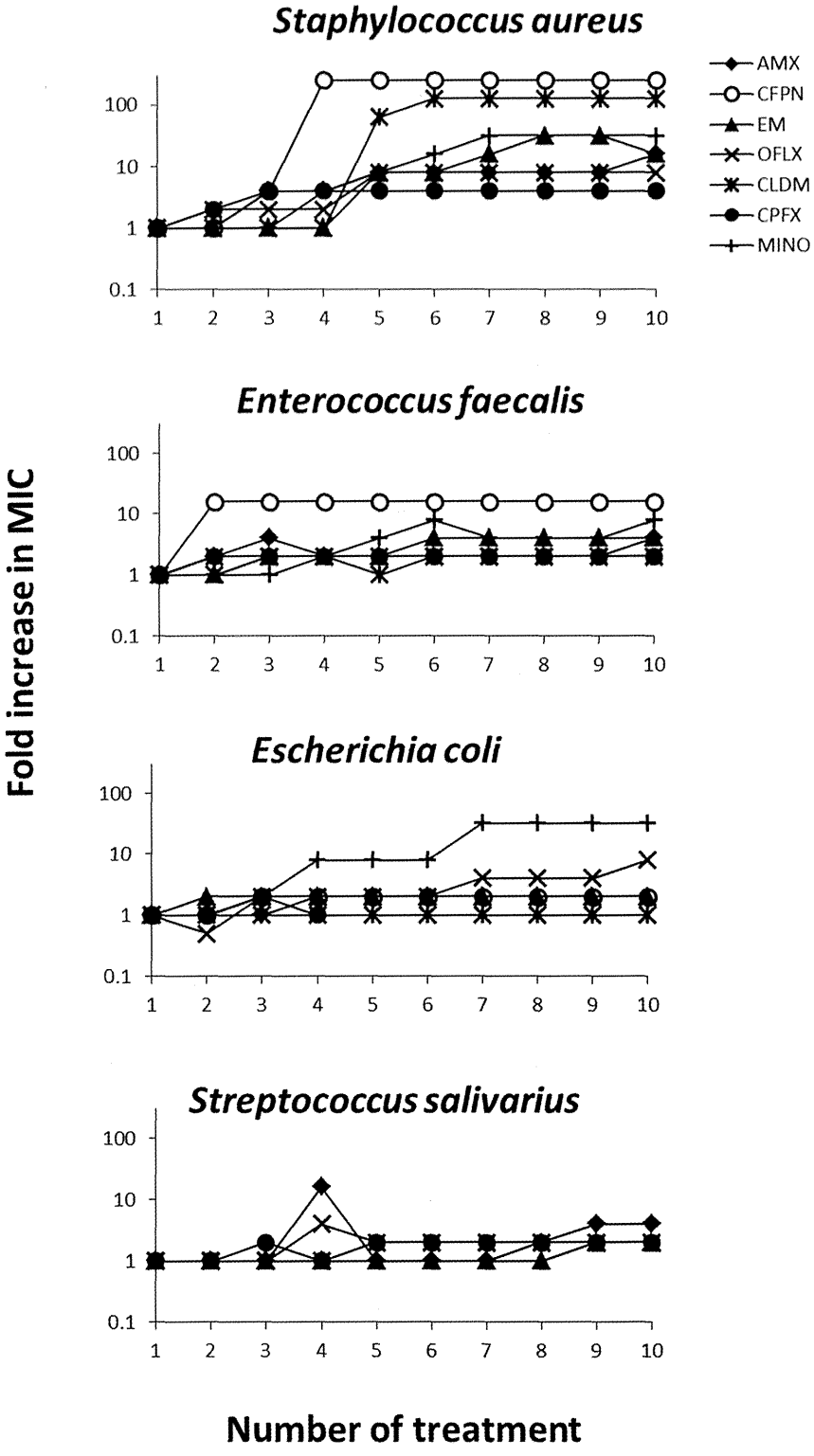

Figure 2. Fold increases in MICs of antibacterial agents against four bacterial species during exposure to these agents. Each bacterial species was exposed 10 times. Each initial MIC is regarded as 1 MIC. Each value represents the mean of duplicate determinations.
doi:10.1371/journal.pone.0081316.g002

a greater or lesser extent, any of the bacterial species tested became resistant to one or more antibacterial agents tested. Under a similar assay protocol, disinfection treatment with photolysis of H_2O_2 did not result in development of resistance to this treatment in any of the four bacterial species, even after 40 exposures. With regard to the other three bacterial species, *P. aeruginosa*, *S. mutans*, and *A. actinomycetemcomitans*, disinfection treatment with photolysis of H_2O_2 also did not lead to development of resistance.

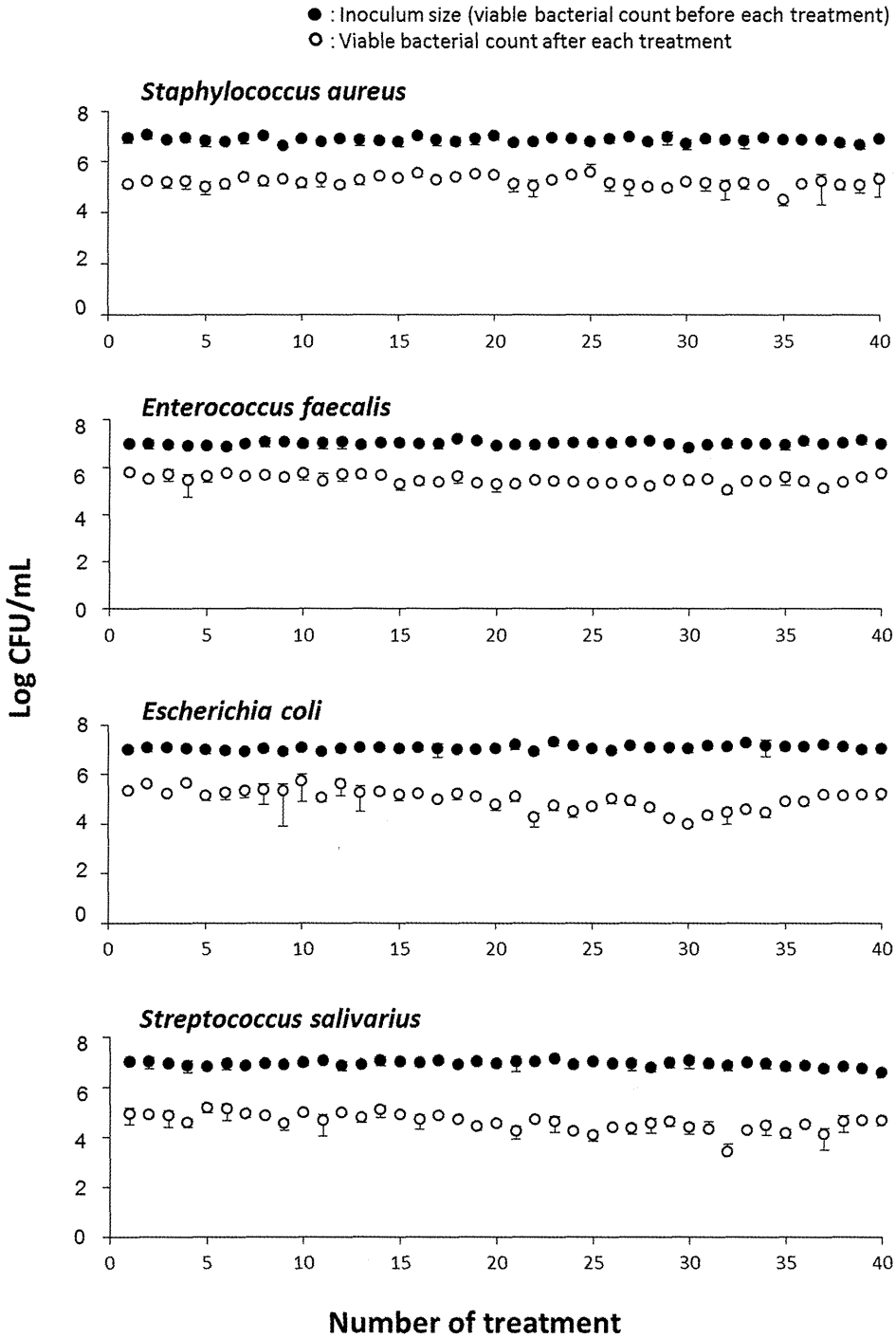

Figure 3. Changes in the antibacterial effect of disinfection treatment with photolysis of H_2O_2 in four bacteria. *Staphylococcus aureus*, *Enterococcus faecalis*, *Escherichia coli*, and *Streptococcus salivarius* were exposed 40 times to disinfection treatment. Each value represents the mean ± standard deviation (n = 3).
doi:10.1371/journal.pone.0081316.g003

Susceptibility of *P. aeruginosa* and *A. actinomycetemcomitans* to repeated treatment of photolysis of H_2O_2 fluctuated compared with the other bacterial species. In the case of *P. aeruginosa*, this was possibly due to a higher sensitivity of this bacterium than that of the other bacterial species. This could be because a laser light irradiation time as short as 10 s was sufficient to achieve a 2-log reduction in viable counts. With regard to *A. actinomycetemcomitans*, one of the possibilities for causing fluctuation might be that the bacterium was cultured under anaerobic conditions following exposure to oxidative stress by hydroxyl radicals, as well as its relatively high sensitivity to disinfection treatment. However, since such fluctuation was not observed in *S. mutans* which was also cultured under anaerobic conditions, effect of anaerobic culture conditions might not be so important.

In general, bacterial resistance is mediated through inactivation of drugs, mutation of active sites of drugs, and/or inhibition of

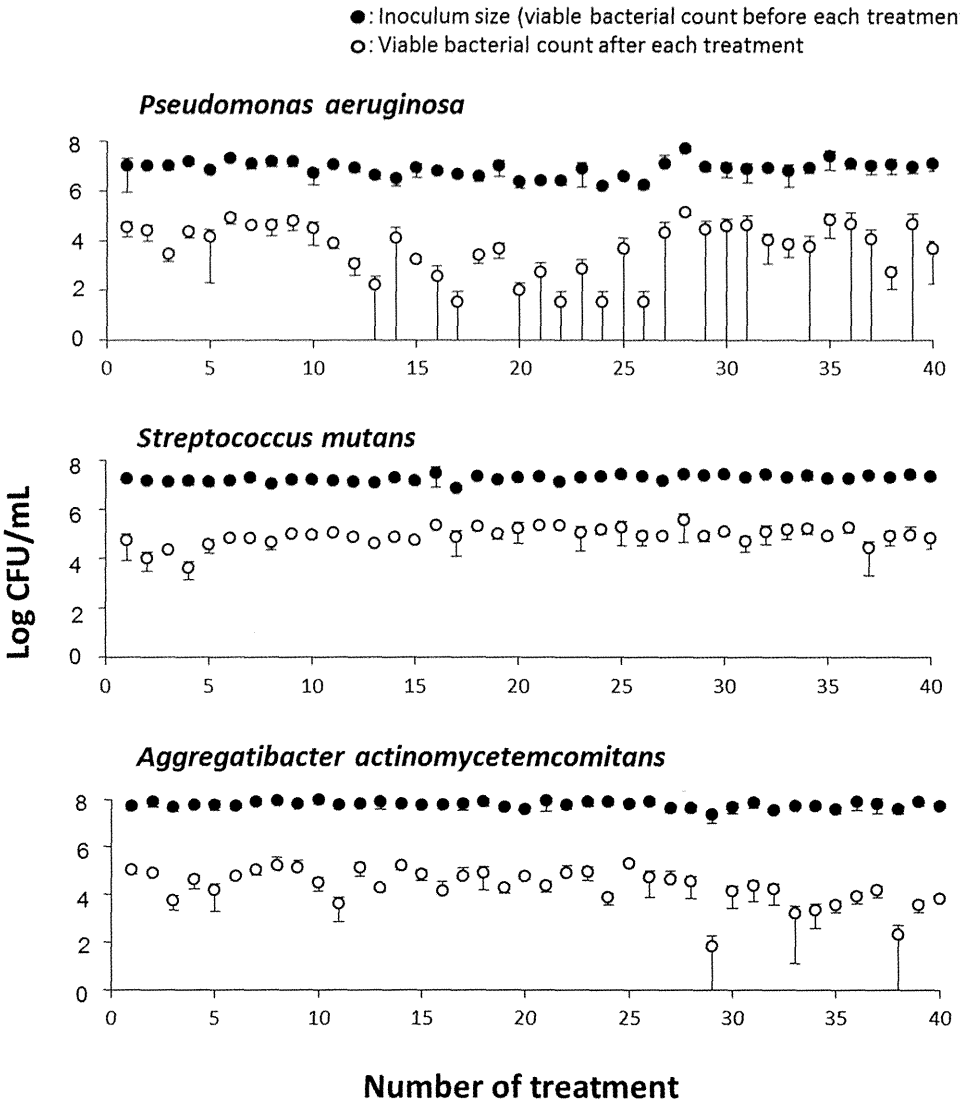

Figure 4. Changes in the antibacterial effect of disinfection treatment with photolysis of H_2O_2 in three bacteria. *Pseudomonas aeruginosa, Streptococcus mutans,* and *Aggregatibacter actinomycetemcomitans* were exposed 40 times to disinfection treatment. Each value represents the mean ± standard deviation (n = 3).
doi:10.1371/journal.pone.0081316.g004

drug-accession to active sites. In addition, bacteria resistant to more than two classes of antibiotics, which are categorized as multidrug resistant, have become a serious problem in the hospital environment. Multidrug resistance may be mediated by extra-chromosomal genetic elements or by overexpression of resistance genes in response to selective pressure [18]. In contrast to susceptibility testing for antimicrobial agents, repeated exposure of the seven bacterial species to disinfection treatment with photolysis of H_2O_2 did not decrease bacterial susceptibility to this treatment. This finding suggests that the risk of inducing bacterial resistance by disinfection treatment is low. In the case of photodynamic antimicrobial chemotherapy (PACT) in which exposure of a photosensitizer to light results in the formation of oxygen species (e.g., singlet oxygen and free radicals), causing microbial cell death, the development of resistance to photodynamic antimicrobial chemotherapy appears to be unlikely. This situation occurs because, in microbial cells, singlet oxygen and free radicals interact with several cell structures and different metabolic pathways [7]. The active ingredient of the disinfection treatment in the present study was the hydroxyl radical, which was laser irradiation time-dependently generated by photolysis of H_2O_2, but not H_2O_2, because exposure of bacteria to 3% (w/v) H_2O_2 without laser irradiation for up to 120 s did not show any bactericidal effect. In studies on PACT, Guiliani et al. studied the possible development of bacterial resistance to PACT after 20 treatments in three major human pathogens, *P. aeruginosa*, *S. aureus*, and *Candida albicans* [10]. All samples were illuminated with a fluence rate of 50 mW/cm^2 for 10 min, and the condition allowed the pathogens survive the PACT. They demonstrated that 20 consecutive PACT treatments did not result in any resistant mutants. Similarly, Tavares et al. demonstrated that the bacteria did not develop resistance to the photodynamic process [9]. In their study, *Vibrio fischerithe* and *E. coli* were subjected to 10 repeated PACT. In their PACT with white light irradiation at 40 W/m^2 for 25 min, 1 log unit of surviving bacteria was achieved. In our study, the disinfection treatment with photolysis of H_2O_2 was carried out on the second time scale. Since we have developed the disinfection treatment with photolysis of H_2O_2 to achieve highly effective bactericidal activity, the

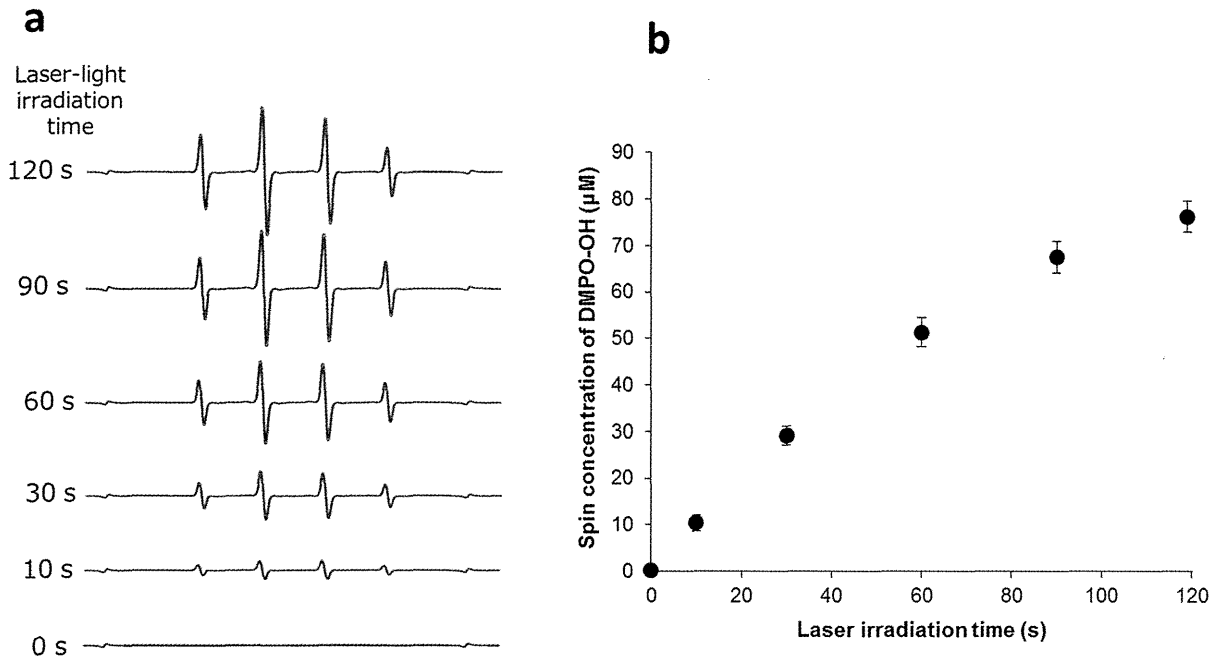

Figure 5. Representative ESR spectra and the yield of DMPO-OH obtained by laser-light irradiation of 3% H_2O_2. (a) ESR spectra and (b) DMPO-OH yields are shown. Each value in (b) represents the mean ± standard deviation (n = 3).
doi:10.1371/journal.pone.0081316.g005

disinfection treatment applied in the present study has an ability to kill pathogenic bacteria including *S. aureus* and *E. faecalis* with a >5-log reduction of viable counts within 3 min [1], indicating that it is difficult to get bacteria surviving the disinfection treatment after 3 min treatment. To evaluate the risk of inducing bacterial resistance, surviving bacteria is needed to be subcultured for the next passage. That is a reason for that the treatment was carried out on the second time scale up to 120 s. To study the risk of developing bacterial resistance in this manner, not only the disinfection treatment with photolysis of H_2O_2 but also PACT was set to exert sublethal effect by controlling the treatment time although the disinfection treatment in the present study was carried out on the second time scale and PACT on the minute time scale. Thus despite the somewhat difference in the treatment time between the two, it is assumed that the experimental conditions were comparable each other. Therefore, as is the case with PACT, it was expected that no bacterial resistance was induced by hydroxyl radicals. Anti-oxidant enzymes, such as superoxide dismutase and catalase, protect against some reactive oxygen species, but not against hydroxyl radicals. There is the possibility that catalase in bacterial cells may affect H_2O_2, resulting in a reduced amount of hydroxyl radicals. However, this would be negligible because 3% H_2O_2 is a high enough concentration that bacteria should not be degraded by their inherent catalase. To further confirm the low risk of developing bacterial resistance, more bacterial strains including drug resistant mutants should be evaluated since only one strain of each bacterial species was tested in the present study.

Considering the emergence of antibiotic-resistant strains in recent years, disinfection treatment with photolysis of H_2O_2 appears to be a potential alternative for existing antimicrobial agents because of its low risk of inducing bacterial resistance.

Author Contributions

Conceived and designed the experiments: YN TK KN KS. Performed the experiments: HI YO KN MS. Analyzed the data: YN HI KN. Contributed reagents/materials/analysis tools: HI YO KN MS. Wrote the paper: YN.

References

1. Ikai H, Nakamura K, Shirato M, Kanno T, Iwasawa A, et al. (2010) Photolysis of hydrogen peroxide, an effective disinfection system via hydroxyl radical formation. Antimicrob Agents Chemother 54: 5086–5091.
2. Shirato M, Ikai H, Nakamura K, Hayashi E, Kanno T, et al. (2012) Synergistic effect of thermal energy on bactericidal action of photolysis of H_2O_2 in relation to acceleration of hydroxyl radical generation. Antimicrob Agents Chemother 56: 295–301.
3. FAD (2003) FR Doc 03-127835.
4. Hayashi E, Mokudai T, Yamada Y, Nakamura K, Kanno T, et al. (2012) *In vitro* and *in vivo* anti-*Staphylococcus aureus* activities of a new disinfection system utilizing photolysis of hydrogen peroxide. J Biosci Bioeng 114: 193–197.
5. American Society for Microbiology, A. S. f. (1995) Report of the ASM Task Force on Antibiotic Resistance. Washington, DC: American Society for Microbiology.
6. Russell AD, Day MJ (1996) Antibiotic and biocide resistance in bacteria. Microbios 85: 45–65.
7. Konopka K, Goslinski T (2007) Photodynamic therapy in dentistry. J Dent Res 86: 694–707.
8. Pedigo LA, Gibbs AJ, Scott RJ, Street CN (2009) Absence of bacterial resistance following repeat exposure to photodynamic therapy. Proc SPIE 7380: 73803H.
9. Tavares A, Carvalho CM, Faustino MA, Neves MG, Tome JP, et al. (2010) Antimicrobial photodynamic therapy: study of bacterial recovery viability and potential development of resistance after treatment. Mar Drugs 8: 91–105.
10. Giuliani F, Martinelli M, Cocchi A, Arbia D, Fantetti L, et al. (2010) In vitro resistance selection studies of RLP068/Cl, a new Zn(II) phthalocyanine suitable for antimicrobial photodynamic therapy. Antimicrob Agents Chemother 54:637–642.
11. Eick S, Schmitt A, Sachse S, Schmidt KH, Pfister W (2004) *In vitro* antibacterial activity of fluoroquinolones against *Porphyromonas gingivalis strains*. J Antimicrob Chemother 54: 553–556.
12. Fujita K, Tanaka N, Orihara K, Noguchi M, Takizawa T, et al. (2010) Studies on effects of various antimicrobial agents on acuisition of resistance in *Staphylococcus aureus*. Rinsho Iyaku 26: 483–487. (in Japanese)
13. Tambe SM, Sampath L, Modak SM (2001) *In vitro* evaluation of the risk of developing bacterial resistance to antiseptics and antibiotics used in medical devices. J Antimicrob Chemother 47: 589–598.

14. CLSI M7-A7 (2006) Methods for dilution antimicrobial susceptibility tests for bacteria that grow aerobically; approved standard-seventh edition
15. Watanakunakorn C (1988) *In-vitro* induction of resistance in coagulase-negative staphylococci to vancomycin and teicoplanin. J Antimicrob Chemother 22: 321–324.
16. Nakamura K, Kanno T, Ikai H, Sato E, Mokudai T, et al. (2010) Reevaluation of quantitative ESR spin trapping analysis of hydroxyl radical by applying sonolysis of water as a model system. Bull Chem Soc Jpn 83: 1037–1046.
17. Buettner GR (1987) Spin trapping: ESR parameters of spin adducts. Free Radic Biol Med 3: 259–303.
18. Mallik D, Kumar A, Sarkar SK, Ghosh AS (2013) Multiple Resistance Mechanisms Acting in Unison in an Escherichia coli Clinical Isolate. Curr Microbiol. Epub ahead of print.

Langmuir

Article

pubs.acs.org/Langmuir

Molecular Interaction Forces Generated during Protein Adsorption to Well-Defined Polymer Brush Surfaces

Sho Sakata,[†] Yuuki Inoue,*[,†] and Kazuhiko Ishihara*[,†,‡]

[†]Department of Materials Engineering and [‡]Department of Bioengineering, School of Engineering, The University of Tokyo 7-3-1, Hongo, Bunkyo-ku, Tokyo 113-8656, Japan

Supporting Information

ABSTRACT: The molecular interaction forces generated during the adsorption of proteins to surfaces were examined by the force-versus-distance (f–d) curve measurements of atomic force microscopy using probes modified with appropriate molecules. Various substrates with polymer brush layers bearing zwitterionic, cationic, anionic, and hydrophobic groups were systematically prepared by surface-initiated atom transfer radical polymerization. Surface interaction forces on these substrates were analyzed by the f–d curve measurements using probes with the same polymer brush layer as the substrate. Repulsive forces, which decreased depending on the ionic strength, were generated between cationic or anionic polyelectrolyte brush layers; these were considered to be electrostatic interaction forces. A strong adhesive force was detected between hydrophobic polymer brush layers during retraction; this corresponded to the hydrophobic interaction between two hydrophobic polymer layers. In contrast, no significant interaction forces were detected between zwitterionic polymer brush layers. Direct interaction forces between proteins and polymer brush layers were then quantitatively evaluated by the f–d curve measurements using protein-immobilized probes consisting of negatively charged albumin and positively charged lysozyme under physiological conditions. In addition, the amount of protein adsorbed on the polymer brush layer was quantified by surface plasmon resonance measurements. Relatively large amounts of protein adsorbed to the polyelectrolyte brush layers with opposite charges. It was considered that the detachment of the protein after contact with the polymer brush layer hardly occurred due to salt formation at the interface. Both proteins adsorbed significantly on the hydrophobic polymer brush layer, which was due to hydrophobic interactions at the interface. In contrast, the zwitterionic polymer brush layer exhibited no significant interaction force with proteins and suppressed protein adsorption. Taken together, our results suggest that to obtain the protein-repellent surfaces, the surface should not induce direct interaction forces with proteins after contact with them.

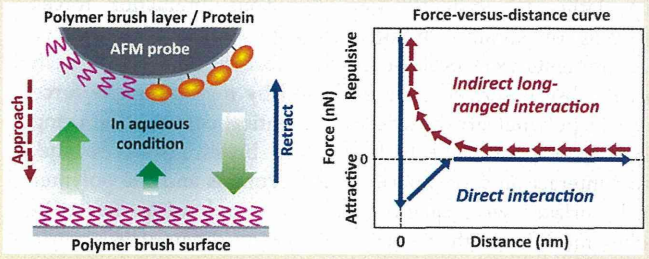

1. INTRODUCTION

A series of biological reactions progresses hierarchically at interfaces between biomolecules and the surface with which they interact. Protein adsorption on the surfaces of materials is an initial reaction and is generally induced immediately. The amount of adsorbed protein and its conformational change are significant factors that determine the subsequent biological responses at cellular and tissue levels.[1−3] Therefore, protein adsorption to surfaces should be completely understood and regulated for developing safer and more efficacious medical devices and maintaining cell function in order to fully achieve regenerative medicine. Protein adsorption depends on various intermolecular/surface interaction forces operating between the material surface and proteins.[4,5] Much research has elucidated protein adsorption behavior in the context of physicochemical surface properties by using the water contact angle or surface ζ-potential as parameters. However, analyses concerning the strength or range of such interaction forces have been relatively limited. The objective of this study was to clarify the protein adsorption process from the perspective of molecular interaction forces operating on surfaces.

Generally, electrostatic and hydrophobic forces are considered to be the main driving forces for protein adsorption on surfaces. However, it is difficult to precisely distinguish these interaction forces in the case of conventional polymeric surfaces or polymer-coated surfaces because of their vague arrangement of polymer chains. Therefore, in the present study we utilized polymer brush surfaces prepared via the surface-initiated atom transfer radical polymerization (SI-ATRP) method.[6−12] In SI-ATRP, monomers are uniformly polymerized from surface-immobilized initiators, which enable the construction of homogeneous polymer layers composed of a single monomer unit on the surfaces of various substrates. Moreover, the surface's physicochemical properties (hydrophilicity/hydrophobicity and surface potential) can be controlled over a wide range by varying the chemical structure of monomer units.[13−15] Thus, the clarification of surface interaction forces would be enhanced by utilizing polymer brush surfaces

Received: January 28, 2015

ACS Publications © XXXX American Chemical Society

DOI: 10.1021/acs.langmuir.5b00351
Langmuir XXXX, XXX, XXX−XXX

prepared from systematically selected monomers (for example, zwitterionic, cationic, anionic, and hydrophobic).

Atomic force microscopy (AFM) is used to quantitatively analyze the various molecular interaction forces on surfaces.[16] In the force-measurement mode of AFM, the interaction force operating between the probe and a sample is acquired as a function of the distance between them, generating a force-versus-distance (f–d) curve. Therefore, AFM enables the detection of long-range interactions operating prior to contact between the probe and the sample as well as the direct interaction forces operating after contact. Moreover, various interaction forces can be evaluated by modification of the probe with appropriate molecules, including peptides, proteins, and polymers.[17−20] The combination of fabrication of well-defined polymer brush surfaces and nanoforce analysis by AFM would help clarify our understanding of various interaction forces operating on surfaces. In this study, two types of f–d curve measurements were performed. First, forces operating on each polymer brush surface were evaluated by measuring the force between polymer brush surfaces of identical composition using AFM probes modified with polymer brush layers. Second, direct interaction forces between the proteins and the polymer brush surfaces were quantitatively evaluated using the AFM probes modified with two proteins having different isoelectric points (pI's) and opposite net charges under physiological conditions. Furthermore, the amounts of these proteins adsorbed on the polymer brush surfaces were quantified, and the relationship among surface interaction forces, the surface–protein direct interaction force, and protein adsorption behavior is discussed.

2. EXPERIMENTAL SECTION

2.1. Materials. 2-Methacryloyloxyethyl phosphorylcholine (MPC) was purchased from NOF (Tokyo, Japan), which was synthesized and purified according to a previously reported method.[21] 2-Trimethylammoniumethyl methacrylate chloride (TMAEMA) and 3-sulfopropyl methacrylate potassium salt (SPMA) were purchased from Tokyo Chemical Industry (Tokyo, Japan). n-Butyl methacrylate (BMA) was purchased from Kanto Chemical (Tokyo, Japan). Copper(I) bromide (CuBr) and 2,2′-bipyridyl (Bpy) were purchased from Wako Pure Chemical Industries (Osaka, Japan). Ethyl-2-bromoisobutyrate (EBIB), 4,4′-dinonyl-2,2′-bipyridyl (DNbpy), bovine serum albumin, and chicken egg white lysozyme were purchased from Sigma-Aldrich (St. Louis, MO, USA). Other organic reagents and solvents were commercially available in extra-pure grade and used without further purification. Silicon wafers were purchased from Furuuchi Chemical (Tokyo, Japan); their surfaces were coated with ~10-nm-thick SiO_2 layers.

2.2. Preparation of Polymer Brush Surfaces. Polymer brush layers were prepared on the initiator-immobilized substrates by SI-ATRP using MPC, TMAEMA, SPMA, and BMA according to a previously reported procedure.[22] Briefly, a surface-immobilizing initiator, (10-(2-bromo-2-methyl)propionyloxy)decyltrichlorosilane (BrC10TCS), was synthesized and immobilized on the silicon substrates as previously described.[23] Specific amounts of the monomer, CuBr, and Bpy were dissolved in degassed solvents. Potassium chloride of the same concentration as SPMA (0.50 mol/L) was added to the SPMA solution to enhance the solubility of SPMA. DNbpy was used as the ligand instead of Bpy for the polymerization of BMA. Then, the BrC10TCS-immobilized substrates and EBIB, as the free initiator, were simultaneously placed into the solution to initiate SI-ATRP. Polymerization was performed with stirring at 20 °C for 24 h. The target degree of polymerization (DP, [monomer]/[free initiator] ratio in the feed) was set at 100. The conversion of monomer to polymer was determined by proton nuclear magnetic resonance spectroscopy (^{1}H NMR) (α-300; JEOL, Tokyo, Japan).

The surface elemental composition of the polymer brush surface was determined by X-ray photoelectron spectroscopy (XPS) (AXIS-Hsi; Shimadzu/Kratos, Kyoto, Japan). The thickness of the polymer brush layer was measured by spectroscopic ellipsometry (α-SE; J.A. Woolam, Lincoln, NE, USA) and was determined using the Cauchy layer model with an assumed refractive index of 1.49 at 632.8 nm. The graft density, σ (chains/nm^2), was calculated using the following equation: $\sigma = h\rho N_A/M_n$, where h (nm) is the ellipsometric thickness of the polymer brush layer, ρ (g/cm^3) is the density of the dry polymer, N_A is Avogadro's number, and M_n is the number-average molecular weight of polymer on the surface. M_n was assumed to be the same as the number-average molecular weight of each polymer in the polymerization solution,[24,25] which was estimated from the degree of polymerization determined by the ^{1}H NMR spectrum of each free polymer. The static air contact angle on the polymer brush surface in pure water and phosphate-buffered solution (PBS; pH 7.4, ionic strength (I) = 150 mmol/L) was measured at room temperature by the captive bubble method using a goniometer (CA-W; Kyowa Interface Science, Saitama, Japan). The supplementary angles (180°−θ) of the static air contact angles (θ) are shown for easy comparison with static water contact angles under dry conditions. The ζ-potential of the polymer brush surface was measured with an electrophoretic light-scattering spectrophotometer (ELS-8000; Otsuka Electronics, Osaka, Japan) equipped with a planar sample cell in water containing 10 mmol/L sodium chloride at room temperature. The chemical structures of the polymer brush layers are shown in Figure 1.

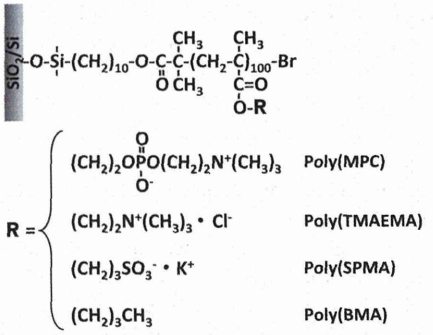

Figure 1. Chemical structures of polymer brush layers.

2.3. Surface Force Analysis. The surface interaction forces at the polymer brush layers were analyzed by f–d curve measurements between polymer brush layers of identical composition (symmetric system) using an AFM equipped with a liquid cell (Nanoscope IIIa; Bruker AXS K.K., Kanagawa, Japan). The essential experimental process is illustrated in Figure 2(a). The polymer brush layers were constructed on the surfaces of silica beads (20 μm diameter, Duke Scientific Co., Palo Alto, CA, USA) using the same method as for the silicon substrates. One silica bead with a polymer brush layer was manually immobilized at the end of a commercial, tipless AFM probe (NP-O; nominal spring constant 0.06 N/m, Bruker AXS K.K.) using a

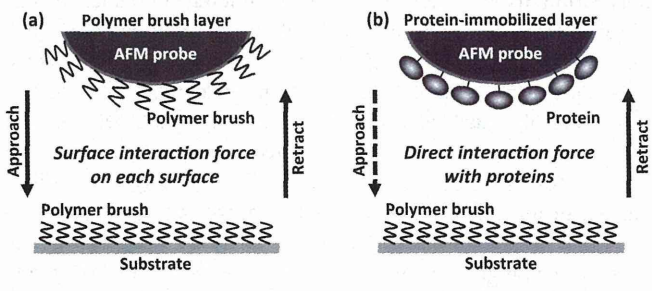

Figure 2. Schematic representation of interaction force measurements by AFM using probes modified with (a) polymer brush layers and (b) a protein-immobilized layer.

DOI: 10.1021/acs.langmuir.5b00351
Langmuir XXXX, XXX, XXX−XXX

small amount of epoxy resin according to a previously reported procedure.[26] The successful immobilization of a silica bead on the probe was confirmed by optical microscopy. The $f-d$ curve measurement was performed using these probes and the polymer brush substrates, and the $f-d$ curves on approach and retraction of the symmetric polymer brush surfaces were recorded in aqueous media with different ionic strengths.

2.4. Quantitative Evaluation of Surface–Protein Interaction Forces. The direct interaction force between the proteins and the polymer brush layers was quantitatively evaluated by $f-d$ curve measurements using an AFM equipped with a liquid cell. The experimental process is illustrated in Figure 2(b). Proteins were chemically immobilized on the surface of the AFM probe (OTR8; nominal spring constant 0.15 N/m, Bruker AXS K.K.) according to a previously reported method.[27] Briefly, 3-nm-thick chromium and sequential 27-nm-thick gold were sputtered on the surface of the probe. The gold-sputtered probe was then immersed in a 1.0 mmol/L solution of 11-mercaptoundecanoic acid in ethanol for 24 h to form a carboxyl-group-terminated self-assembled monolayer on the probe. The carboxyl groups were activated by immersion in an aqueous solution containing *N*-hydroxysuccinimide (50 mmol/L) and 1-ethyl-3-(3-(dimethylamino)propyl)carbodiimide hydrochloride (100 mmol/L). After immersion for 30 min, the probe was rinsed with pure water and immediately immersed in a PBS (pH 7.4, 150 mmol/L) solution of albumin (1.0 mg/mL) or lysozyme (0.10 mg/mL) for 1 h. The immobilization of each protein on the surface was confirmed by XPS and surface plasmon resonance (SPR) (SPR-670M; Moritex, Tokyo, Japan) measurements using gold-sputtered silicon substrates and SPR sensor chips, respectively, instead of the AFM probe. The direct interaction force between the proteins and the polymer brush layers in PBS (pH 7.4, I = 150 mol/L) at room temperature was evaluated from the approaching and retracting traces of the $f-d$ curve using the protein-immobilized probes. The shift in the deflection value of the retracting trace from the bottom of the retrace line corresponds to the interaction force between the proteins and surfaces. For each measurement, more than 100 approaching/retracting $f-d$ curves were collected, and the average value was defined as the interaction force between proteins and the polymer brush layers. All measurements were performed at least three times.

2.5. Evaluation of Protein Adsorption Mass. The amount of albumin (pI 4.8) and lysozyme (pI 11.1) adsorbed on the surfaces of polymer brush layers in PBS (pH 7.4, I = 10, 150 mmol/L) at 37 °C was quantified by SPR measurement.[28] The polymer brush layers were prepared on SPR sensor chips by SI-ATRP using 11-(2-bromo-2-methylpropyonyloxy)undecylmercaptan (BUM) as the surface-immobilizing initiator for the thin gold layer on the substrate.[29] A peristaltic pump (Tokyo Rika Kikai, Tokyo, Japan) was used to flow the buffer solution or protein solution through the SPR sensor surfaces at a rate of 500 μL/min. First, a stable baseline signal was established by flowing buffer solution for 10 min. Then, a 1.0 mg/mL protein solution was flowed for 30 min, followed by buffer solution for 10 min to replace the protein solution, wash off the weakly adsorbed proteins from the surface, and re-establish the baseline.

The amount of adsorbed protein, Γ_{SPR} (ng/cm^2), was estimated using the following relationship:[30] $\Gamma_{SPR} = 500 \times \Delta R_{deg}$, where ΔR_{deg} (deg) is the change in the resonance angle before and after protein adsorption. All measurements were performed at least three times.

3. RESULTS AND DISCUSSION

3.1. Characteristics of Polymer Brush Surfaces. In this study, four different types of polymer brush layers, including electrically neutral (zwitterionic), electrolytic (cationic and anionic), and hydrophobic polymers, were prepared to evaluate the various interaction forces generated on these surfaces. The surface elemental composition of the polymer brush layer was evaluated by XPS (XPS spectra are shown in Figure S1 of the Supporting Information). Every polymer brush layer had corresponding elemental peaks expected from the chemical structure of the monomers. Thus, we confirmed that the surface of the substrate was covered with the polymer brush layer. The physicochemical properties of the polymer brush layers are summarized in Table 1. The graft density (density of the polymer chains in a polymer brush layer) of these polymer brush layers was sufficiently high to form a high-density polymer brush structure.[6] The air contact angles on the polymer brush layers in pure water were below 20° for the poly(MPC), poly(TMAEMA), and poly(SPMA) brush layers. That is, these polymer brush layers exhibited a superhydrophilic nature in an aqueous environment. The hydrophilicities of these surfaces were virtually identical regardless of the ionic strength of the medium. In the case of the poly(BMA) brush layer bearing hydrophobic groups, the air contact angle was approximately 75° and did not depend on the ionic strength, which is consistent with its relatively hydrophobic characteristics. The surface ζ-potential values reflected the charge properties of the side chains of each polymer brush layer. That is, the cationic poly(TMAEMA) brush layer had a large positive value whereas the anionic poly(SPMA) brush layer had a large negative value. The poly(MPC) brush layer with zwitterionic phosphorylcholine groups had an almost neutral value. As described above, we confirmed that the systematic model surfaces were prepared from the perspective of the physicochemical surface properties.

Table 1. Physicochemical Properties of Polymer Brush Layers

polymer brush layer	graft density (chains/nm^2)	contact angle of air (deg)		ζ-potential (mV)
		in water	in PBS	
poly(MPC)	0.33	9 ± 2	9 ± 1	−5.9 ± 2.1
poly(TMAEMA)	0.45	17 ± 0	14 ± 0	64.9 ± 3.6
poly(SPMA)	0.55	13 ± 2	12 ± 1	−74.0 ± 11.7
poly(BMA)	0.75	73 ± 3	74 ± 1	−37.2 ± 6.1

3.2. Surface Interaction Force. To clarify the surface interaction forces on each of the polymer brush surfaces, $f-d$ curve measurements between polymer brush layers of identical composition were performed with a focus on the approaching and retracting processes. Figure 3 shows the representative $f-d$ curves recorded for the approaching process of the symmetric poly(MPC), poly(TMAEMA), and poly(SPMA) brush layers. The same procedure was repeated with different ionic strengths of the medium. On the zwitterionic poly(MPC) brush layer, only weak repulsive forces were detected, and these forces were independent of the ionic strength in solution. That is, a specific interaction force was not detected on the poly(MPC) brush layer. On the cationic poly(TMAEMA) and the anionic poly(SPMA) brush layers, strong repulsive forces were detected at long distances in pure water. The strength and range of these forces decreased with increasing ionic strength in solution. Therefore, these repulsions were mainly derived from electrostatic forces. We conclude that electrostatic interactions were predominantly operating on the poly(TMAEMA) and the poly(SPMA) brush layers. It is well known that the charge effects of polyelectrolytes in aqueous media are shielded by the addition of salt. The same phenomenon was observed at the polymer brush layer. Figure 4 shows the representative $f-d$ curves recorded for the retracting process of the symmetric poly(MPC), poly(TMAEMA), and poly(SPMA) brush layers

DOI: 10.1021/acs.langmuir.5b00351
Langmuir XXXX, XXX, XXX–XXX